

Measurement of Very Weak Light Signals and Spectra

To cite this article: Humio Inaba *et al* 1975 *Jpn. J. Appl. Phys.* **14** 23

View the [article online](#) for updates and enhancements.

You may also like

- [Probing Dark Energy and Modifications of Gravity with Ground-based millimeter-wavelength Line Intensity Mapping](#)
Azadeh Moradinezhad Dizgah, Emilio Bellini and Garrett K. Keating
- [Fiber-end antireflection method for ultra-weak fiber Bragg grating sensing systems](#)
Zhihui Luo, Yu Zhang, Wensheng Cheng et al.
- [Flexible UV detectors based on *in-situ* hydrogen doped amorphous Ga₂O₃ with high photo-to-dark current ratio](#)
Yanxin Sui, Huili Liang, Wenxing Huo et al.

Measurement of Very Weak Light Signals and Spectra

Humio INABA, Yoshiaki SHIMIZU and Yasuhiro TSUJI

*Research Institute of Electrical Communication, Tohoku University,
Katahira 2-Chome, Sendai 980*

This paper reviews briefly the photoelectric methods for measuring very weak light signals based on the analog and digital techniques. Comparative study performed experimentally and theoretically shows that the single photoelectron counting method is advantageous with regard to sensitivity and stability. As a further extension of this study, the method for measuring the spectral distribution of ultra-low light signals was studied which led to the design and construction of a new type of spectrometer, called the filter spectral analyzer. Experimental tests to examine its performance and comparisons of its sensitivity with a conventional grating spectrometer were made by accomplishing the spectral analysis of low-level light sources. Moreover, as far as we know, the first spectroscopic measurements of the ultra-weak chemiluminescence associated with some sorts of enzymatic reactions were performed successfully as the new application of the measuring methods developed and evaluated in this paper.

§1. Introduction

In a variety of fields in scientific research and applications such as physics, chemistry, space science and technology, and bioscience including medicine and pharmacology, the problem for measuring light intensities and their spectral distribution at very low levels is becoming considerably important. In view of measurements of light in extreme conditions, the systematic study and development of this problem for very weak light signals and spectra from various kinds of faint sources as well as an emitter or a scatterer which releases merely a small amount of photon against a background of much higher intensity are of extreme interest and widely attractive as a new era of optical technology.

This paper is devoted to the description of experimental and theoretical studies on the performance and sensitivity of photoelectric methods for measuring light signals and their spectra carried in the ultra-low photon fluxes of which the power is of the order of less than 10^{-15} W. The first part of the present paper will review briefly the measuring methods of very weak light intensity accomplished by the use of photomultipliers. The analytical results and their comparison on the signal-to-noise ratio for the detection techniques based on analog and digital schemes are presented from a unified viewpoint along with their experimental verification and comparisons.¹⁻⁶⁾ Based on these studies, the measuring techniques for

ultra-low optical signals have already been applied to Raman scattering and nonlinear optics by the present authors.^{1-3,5,6)} Furthermore, we have reported the first successful measurements of extra-weak bioluminescence from living tissues such as tumors and livers of mice and rats as a novel application of these methods.^{5,6)}

The second part of this paper is concerned with the challenge of extracting the spectral information carried in very weak light signals, as a further extension of our previous works. As far as we are aware, no appreciable efforts in research and development on the spectral analysis of ultra-low level light have been performed before. For this aim, we have designed and constructed a new type of spectrometer, called a filter spectral analyzer, by utilizing a set of colored glass filters with different sharp short-wavelength cutoffs to allow the total optical transmission through the apparatus to be as large as possible. Experimental and analytical studies on the performance and sensitivity of this filter spectral analyzer are also described, including a comparison with a conventional grating spectrometer. Furthermore, the first-time measurement of the spectra of extra-weak chemiluminescence accompanied by various kinds of biochemical processes, including autoxidation and enzymatic reaction, is reported to be one of the successful applications of our technique established by the filter spectral analyzer.

Table I. Classification of photoelectric methods for measuring weak light signals.

Classification	Analog scheme		Digital scheme
	DC	AC	Photoelectron pulse
Without synchronous detection	DC method	AC method	SPC method
With synchronous (phase sensitive) detection	SDC method	SAC method	SSPC method

§2. Classification and Sensitivity Comparisons of Measuring Methods for Weak Light Signals

2.1 Classification of photoelectric measuring methods

Two kinds of photoelectric measuring methods are presently being used in common in the spectral region accessible to a photomultiplier (PM); we refer to them as the analog and digital schemes. The analog method is usually divided into two categories; the dc method which is widely used, and the ac method which recovers the desired information by detecting the associated shot noise.^{7,8)} With the digital method, contributions from photoelectrons are resolved in time so that the signals in the form of electron pulses are detected by means of a pulse counting system. This technique is customarily called single photoelectron counting (SPC) or, simply, the photon counting method.^{9,10)} In addition to these basic regimes, a conventional synchronous technique or the phase sensitive detection method can be combined with each of them in order to extract only the signal component buried in a random noise as well as to improve

the sensitivity and the stability. Hence, the measuring methods of weak light signals are conventionally classified into six schemes;^{1,2)} DC and SDC,¹¹⁾ AC and SAC,¹²⁾ and SPC and SSPC,^{13,14)} respectively. Here the first S's refer to the term of synchronous. Table I summarizes the classification of these methods for measuring weak light intensity.

2.2 Theoretical analysis on sensitivity of measurements

The analytical study on the detection sensitivity of these six schemes was performed from a unified point of view, and the quantitative comparison of the signal-to-noise ratio and the minimum detectable optical power was made along with the discussion on the linearity, stability and time response.^{1-3,6)}

Table II is a summary of some essential results based on the analysis with respect to these measuring methods. In this table, the detected light signals are converted into the average number of counts of photoelectron $\langle N_s \rangle$, and of noise current electron $\langle N_n \rangle$ to allow the mutual comparison. The effective range of the signal photoelectron number and the signal-to-noise voltage ratio are expressed

Table II. Classification and comparison of signal-to-noise ratio of DC and SDC, SPC and SSPC methods for detection of ultra-low light intensity.

Classification	Analog detection			
	DC method	SDC method	AC method	SAC method
Effective range	$\langle N_s \rangle > 2B\mu_s$		$\langle N_s \rangle < 2B\mu_s$	
Signal-to-noise voltage ratio	$\frac{\langle N_s \rangle / \sqrt{2b}}{\sqrt{\left\{ \langle N_s \rangle + \langle N_n \rangle \frac{\langle G_n^2 \rangle}{\langle G_s^2 \rangle} \right\} \mu_s}}$	$\frac{\langle N_s \rangle / \sqrt{2b}}{\sqrt{\left\{ \langle N_s \rangle + 4\langle N_n \rangle \frac{\langle G_n^2 \rangle}{\langle G_s^2 \rangle} \right\} \mu_s}}$	$\frac{\langle N_s \rangle / \sqrt{2b}}{\sqrt{\left\{ \langle N_s \rangle + \langle N_n \rangle \frac{\langle G_n^4 \rangle}{\langle G_s^4 \rangle} \right\} \mu'_s}}$	$\frac{\langle N_s \rangle / \sqrt{2b}}{\sqrt{\left\{ \langle N_s \rangle + 4\langle N_n \rangle \frac{\langle G_n^4 \rangle}{\langle G_s^4 \rangle} \right\} \mu'_s}}$

$\langle N_s \rangle, \langle N_n \rangle$: average rate for signal photoelectron and noise pulse.

B, b : bandwidth of amplifier and low pass filter.

$\langle G_s \rangle, \langle G_n \rangle$: average gain of photomultiplier for signal and noise.

μ_s, μ'_s : excess noise factor $\mu_s = \langle G_s^2 \rangle / \langle G_s \rangle^2$, $\mu'_s = \langle G_s^4 \rangle / \langle G_s^2 \rangle^2$.

$\xi(V)$: signal-to-noise counting efficiency ratio.

*It is assumed that the output pulse from a photomultiplier ranges in the single photoelectron event with the

in terms of the detection bandwidth of the amplifier B , average gains $\langle G_s \rangle$ and $\langle G_n \rangle$, and the excess noise factor μ_s and μ'_s in the photomultiplier, the signal-to-noise counting efficiency ratio $\xi(V)$, the bandwidth of the low-pass filter b for the case of analog operation, and the detection time T for the case of digital operation. The signal-to-noise counting efficiency ratio $\xi(V)$ as a function of a selected pulse-height discriminator voltage V is defined by $\xi(V) = \int_V^\infty p_n(v) dv / \int_V^\infty p_s(v) dv$, where $p_s(v)$ and $p_n(v)$ express the pulse-height distribution functions of a signal photoelectron and a dark current pulse, respectively.^{4,5} It is to be noted that the signal-to-noise voltage ratio is defined as the mean signal current or average photoelectron number divided by the standard deviation of the fluctuation of the signal and noise current or the electron number, as it is customarily used. Also, we should point out that the expressions of the signal-to-noise voltage ratio for the three schemes combined with a conventional synchronous method are different only by numerical factors (>1) appearing in the second term of the denominator in each formula.

Figure 1 shows, as an example of our analysis, the theoretical curves of the signal-to-noise voltage ratio as a function of the optical input power at the wavelength of 632.8 nm for three methods without the use of synchronous technique. The average count rate of noise $\langle N_n \rangle$ was assumed to be 50 counts/sec, which is a typical value for the cooled PM such as HTV R376 used for the measurement described below. The SPC method was found to give

AC and SAC, and

Digital detection	
SPC method	SSPC method
$\langle N_s \rangle < 0.1B^*$	
$\frac{\langle N_s \rangle \sqrt{T}}{\sqrt{\langle N_s \rangle + \langle N_n \rangle \xi(V)}}$	$\frac{\langle N_s \rangle \sqrt{T}}{\sqrt{\langle N_s \rangle + 2\langle N_n \rangle \xi(V)}}$

probability, given by $\exp \{-(\langle N_s \rangle + \langle N_n \rangle)/2B\}$, of 95%.

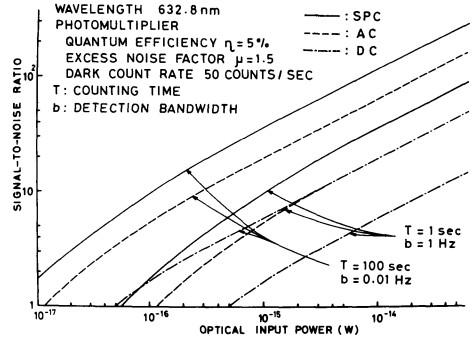


Fig. 1. Theoretical curves showing the relation between the signal-to-noise voltage ratio and the optical input power for three schemes of the photoelectric method including DC, AC and SPC methods. In calculation, the photomultiplier is assumed to have quantum efficiency at 632.8 nm $\eta = 5\%$, excess noise factor $\mu = 1.5$, and average count rates of noise $\langle N_n \rangle = 50$ counts/sec.

better performance than the AC and DC methods, especially in the small input power region, similar to the case of ITT FW130 PM.⁵ With the analog regime, the AC method exceeds by a factor of approximately 3 over the DC method. If one increases the detection time or the time constant of the system, for instance, to 100 sec, this figure shows that the measuring capability extends to 5×10^{-18} W as the minimum detectable power by the use of the SPC method. This minimum value corresponds approximately to one photoelectron per every 2 sec, or 10 photons/sec. The detection of much smaller optical signals could be expected by the use of longer detection or integration time. We note that similar features can also be predicted for the other three methods combined with the synchronous technique.

2.3 Experimental study on sensitivity of measurements

The comparative study of these photodetection methods for weak light signals were also carried out experimentally using a number of well-known PM's suitable for this purpose. As one of the typical results, Fig. 2 shows the measured relation between the signal-to-noise ratio and the optical input power for the case of a cooled HTV R376 with the detection time of 1 sec. The light source employed for this measurement was the standard lamp EOA L-101 with the NBS calibration, incorporated with an interference filter centered at 632.8 nm

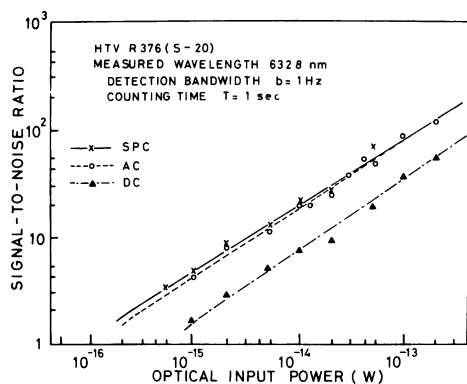


Fig. 2. Measured results of the signal-to-noise voltage ratio as a function of optical input power at 632.8 nm for three measuring methods using a cooled HTV R376 photomultiplier (S-20) with the detection time of 1 sec.

with FWHM of 3 nm and a series of calibrated neutral density filters. It is readily understood that the measurements compare favorably with the theoretical curves depicted in Fig. 1 within a factor of two. Further experimental studies were performed by measuring the Rayleigh scattering intensities and the Raman spectra from various kinds of liquids such as benzene, nitrobenzene and carbon tetrachloride excited by a low-power He-Ne laser.

It is concluded that the general tendency of these experimental results allows us to confirm well our analytical evaluation on measuring methods of weak light signals. In summary, the AC and SAC schemes provide good performance compared with the DC and SDC schemes, although both schemes generally require a rather limited detection time owing to the analog operation. However, the SPC and SSPC methods, which are capable of increasing the counting time and thus of improving the sensitivity, are advantageous over the other methods as far as the measurement of ultra-low light signals is concerned.^{1,3,15,16)}

§3. Measuring Method for Very Weak Light Spectra

3.1 Design and construction of filter spectral analyzer

In order to establish the specific method for the spectral measurement of very weak light signals in conjunction with the single photoelectron counting regime of which potentiality has been demonstrated, we have tried to design and

construct a new type of spectrometer. For this spectrometer, called a filter spectral analyzer, a set of colored glass filters which possesses different sharp short-wavelength cutoffs is utilized instead of a combination of the wavelength dispersion element such as grating or prism and the slit, because it is of primary importance and requisite to minimize the total optical loss of the whole system.

Figure 3 shows the block diagram of the newly developed apparatus based on this principle, including the data processor, for the spectral measurement of ultra-low light signals. Especially, this apparatus is designed for the spectral analysis of a low-level light source with a large emitting area, such as is exhibited by chemiluminescence or bioluminescence, although modification suitable to any other types of light sources can be readily performed. For this purpose, the emitting source is customarily placed in a sample cell of container made of quartz which is controlled at a suitable temperature for the measurement. The emitted optical energy is gathered effectively on the photocathode of the PM which is cooled by vaporized liquid nitrogen by means of an ellipsoidal reflector.

The spectral measurement of very weak light signals is accomplished with the successive insertion of colored glass filters arranged on a rotating disk into the optical path between the reflector and the PM. Twenty-seven colored filters which are commercially available from Toshiba Electric Co. are employed to cover the total wavelength region between 275 and 670 nm with the transmission ranging from 45% to 60%. The insertion is performed automatically by means of a filter drive controller to cover the required range of the spectrum. The optical signals, transmitted through the individual colored filters, are converted into single photoelectron pulses by the PM to be detected by either the SPC or the SSPC method by selecting a mode of the reversible counter with an appropriate detection time. The chopper and the phase shifter depicted in Fig. 3 are customarily used for the SSPC scheme.

The spectral analysis is then carried out by calculating the count rate for the individual spectral window defined by the subtraction of two transmission curves with different sharp

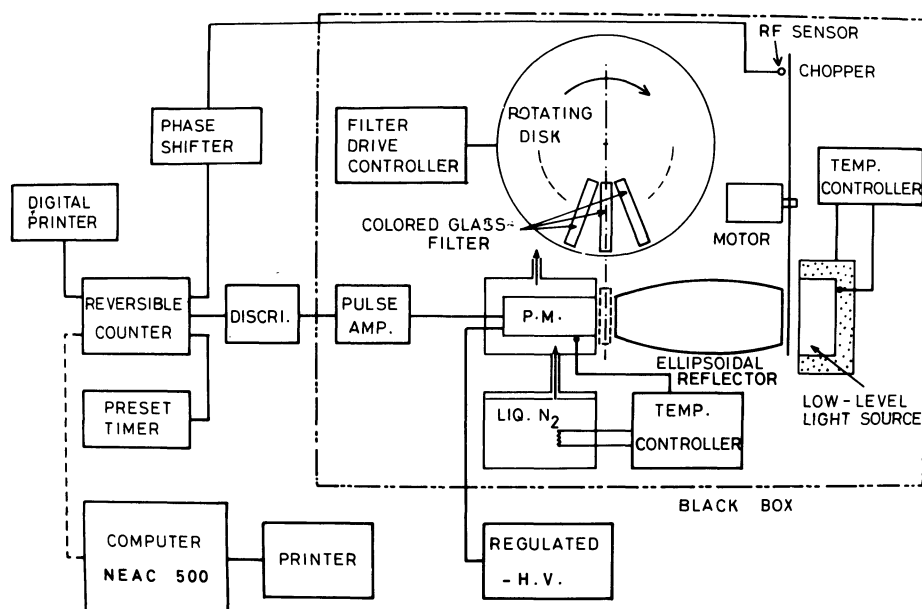


Fig. 3. Block diagram of the new type of spectrometer, the filter spectral analyzer, including data processor, for spectral measurement of very weak light signals incorporated with the digital photoelectron counting method.

short-wavelength cutoffs corresponding to the successive colored glass filters, followed by the calibration of the spectral sensitivity of the photocathode. That is, the average optical intensity P_{ij} between the i th and j th successive colored filters is expressed by

$$P_{ij} = (N_i - N_j) / \int S_k(\lambda) [F_i(\lambda) - F_j(\lambda)] d\lambda, \quad (1)$$

where $N_i - N_j$ is the subtraction of the count rates and $F_i(\lambda) - F_j(\lambda)$ is the subtraction of the transmission curve for the i th and j th successive filters, and $S_k(\lambda)$ means the spectral sensitivity of the PM's photocathode, respectively. This data processing is handled by a digital computer, NEAC-500, either off-line or on-line, to give the spectral information of very weak light signals in the form of a histogram, which can be convoluted by a Lorentzian function representing well the shape of the spectral window, i.e. $F_i(\lambda) - F_j(\lambda)$, when it is necessary. The spectral resolution of this apparatus which depends primarily on the geometry of the individual spectral window is estimated to be 30–50 nm for the wavelength region 275–450 nm and 20–25 nm for the wavelength region 450–670 nm.

Figure 4 shows the external view of the filter spectral analyzer, of which the size is 110 cm in

height, 160 cm in width and 60 cm in length, along with an electric reversible counter, a digital printer and a regulated DC power supply.

3.2 Performance and feasibility of the filter spectral analyzer

For the evaluation of the performance and the operational features of the filter spectral analyzer, experimental comparisons of the sensitivity with a conventional grating spectrometer were performed.

Figure 5 shows one of the typical results of the signal-to-noise ratio as a function of the optical input power for both the filter spectral analyzer and the grating spectrometer with $f/3.5$. For this measurement, the central wavelength of the light source with an aperture of 5 mm diameter was set at 525 nm with a FWHM of 30 nm by the use of an interference filter. Consequently, the resolving power of the grating spectrometer was also arranged to 30 nm to allow us a quantitative comparison. Moreover, as shown in the figure, the measurement was carried out for two different systems, with and without a light collecting device; an ellipsoidal reflector for the former and a lens for the latter.

We note that the filter spectral analyzer with

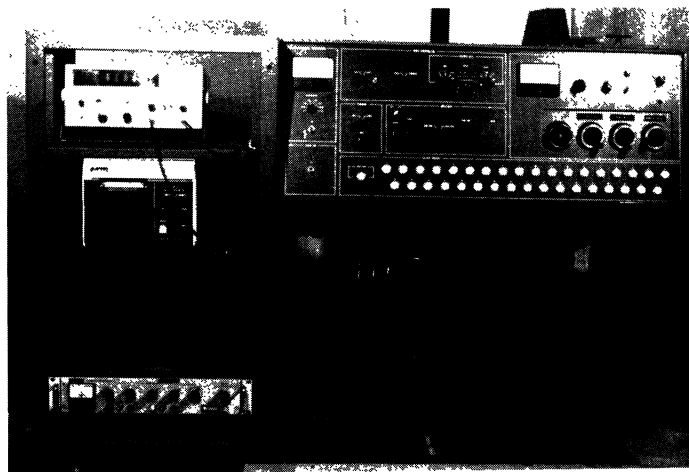


Fig. 4. A photograph of external view of the filter spectral analyzer together with an electric reversible counter, a digital printer and a regulated DC power supply.

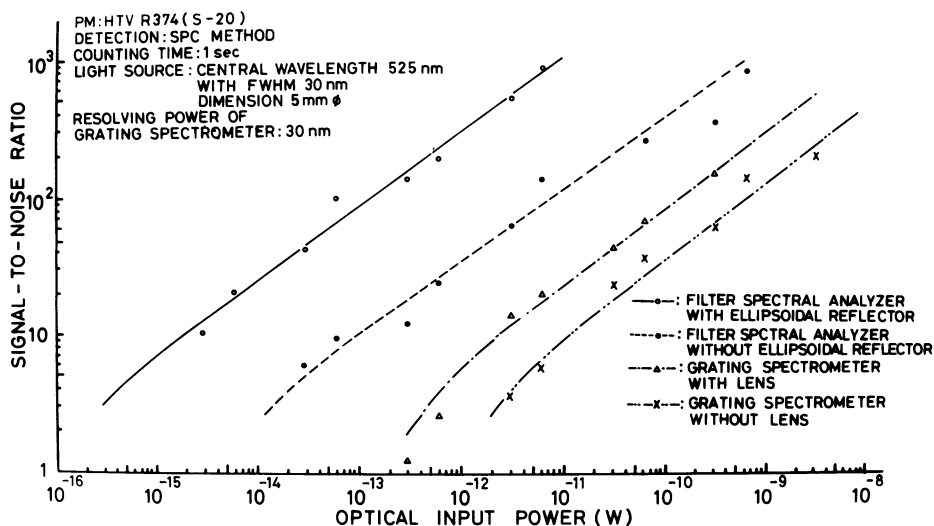


Fig. 5. Comparison of measured sensitivity among the filter spectral analyzer with and without a light collecting ellipsoidal reflector, and a conventional grating spectrometer ($f/3.5$) with and without a lens. In this experiment, as a light source with an aperture of 5 mm in diameter was arranged at 525 nm with FWHM of 30 nm by using an interference filter, the grating spectrometer was also set at 30 nm spectral resolution for the comparison.

the ellipsoidal reflector is superior by about two orders of magnitude to the grating spectrometer with the lens with regard to the sensitivity, but with sacrifice of the spectral resolution. Even for the case without the reflector, it exhibits a better performance by about five times than that of the conventional grating spectrometer with the lens. The minimum detectable optical power for the detection time of 1 sec is estimated to be approximately 10^{-16} W with the spectral resolution of 30 nm for our analyzer incorpo-

rated with the SPC method using HTV R376 which agrees with the result given in Fig. 2. It was also found that the capability of the ellipsoidal reflector as a light collecting device used in this filter spectral analyzer was about eight times more efficient than the case without the reflector in improving the signal-to-noise ratio. Furthermore, the measurements demonstrated that this ellipsoidal reflector can be used for larger dimensions of the light emitting area up to 30 mm in diameter without appreciable

change of the sensitivity of the apparatus.

At this stage, the experimental result will be compared with the analytical estimation based on the following consideration. The spectral instrument is generally assumed to consist of three basic parts; a light source, a spectrometer and a detector. From the Lagrange-Helmholz equation, the interrelationship of these three parts expressed by

$$\Omega_L S_L = \Omega_S S_S = \Omega_D S_D \quad (2)$$

is required for the ideal instrument,¹⁷⁾ where Ω_L , Ω_S and Ω_D are the solid angle of the source and the entrance aperture of the spectrometer and the detector, respectively, and S_L , S_S and S_D are their effective areas. For the grating spectrometer with the lens, the amount of energy per unit time which falls within the detector is given by

$$P_G = L_e \tau_L \tau_G S_G \Omega_G \Delta \lambda_G \quad (3)$$

by assuming eq. (2). Here L_e ($\text{W} \cdot \text{cm}^{-2} \cdot \text{sr}^{-1} \cdot \text{cm}$) is the brightness of the light source, τ_L and τ_G are the transmission coefficients of the lens and the spectrometer, respectively, and $\Delta \lambda_G$ (cm^{-1}) is the resolution of the spectrometer. The solid angle at the entrance aperture in the spectrometer Ω_G (sr) depends on the f number of the spectrometer through the relation

$$\Omega_G = 1/f^2. \quad (4)$$

The effective area of the entrance aperture S_G (cm^2) is also expressed by

$$S = dh, \quad (5)$$

where d (cm) is the width and h (cm) is the height of the entrance slit.

For the filter spectral analyzer with the ellipsoidal reflector, the amount of energy per unit time received by the detector is expressed by

$$P_F = L_e \tau_E \tau_F S_F \Omega_F \Delta \lambda_F, \quad (6)$$

where τ_E and τ_F are the effective transmission coefficients of the ellipsoidal reflector and the colored glass filters, respectively, and $\Delta \lambda_F$ (cm^{-1}) is the resolution of the filter spectral analyzer. In the case of this system, Ω_F (sr) is related to the effective angle θ of the ellipsoidal reflector for collecting the optical energy emitted from a light source through the formula

$$\Omega_F = 2\pi(1 - \cos \theta), \quad (7)$$

and S_F (cm^2) is determined effectively by the

entrance aperture D (cm) of the ellipsoidal reflector as

$$S_F = \pi D^2/4. \quad (8)$$

Using eqs. (3)–(8) and putting $\tau_L \tau_G \simeq \tau_E \tau_F$ and $\Delta \lambda_G \simeq \Delta \lambda_F$ in for comparison, the ratio ζ between the two kinds of the received energy is given by

$$\zeta = \frac{P_F}{P_G} = \frac{\pi^2 D^2 f^2}{2dh} (1 - \cos \theta). \quad (9)$$

If one could assume that the noise generated inside the spectrometer is either mostly the same or negligible for both the spectrometers under consideration, this ratio should provide approximately the improvement factor for the signal-to-noise ratio in our measuring system. For instance, when we suppose $D=3$ cm, $\theta=70^\circ$, $f=3.5$, $d=0.85$ cm, and $h=2$ cm, eq. (9) yields $\zeta=210$ for this factor. This evaluation seems to fall fairly well within the same order of magnitude as the experimental results shown in Fig. 5.

Further experimental tests to confirm the performance of the apparatus were made by accomplishing the spectral analysis of the low-level light sources with well-known spectral distributions such as a low pressure mercury lamp, and a luminol and hydrogen peroxide system in alkali solution accompanying the chemiluminescence through the reaction, of which the total optical power is of the order of 10^{-15} – 10^{-16} W.

Figure 6 illustrates the experimental comparison between the spectroscopic data of the chemiluminescence in the luminol-hydrogen peroxide system obtained by our spectral analyzer and a conventional grating spectrometer. In the upper part of the figure, both of the relative distributions of the spectra are depicted; one is measured at the total input power of 10^{-15} W by the former with the average resolution of 30 nm, and the other is at about 10^{-13} W by the latter with the spectral resolution fixed at 30 nm. The general tendency of agreement between them is readily seen, although the detection times of the SPC scheme were set at 8 sec and 10 sec, respectively. For the reference of the spectral intensity, another two traces of the measured spectrum at the total power of 3×10^{-14} and 10^{-14} W by the grating spectrometer are also shown.

§4. Spectral Measurements of Extra-Weak Spontaneous Chemiluminescence

As a novel application of this method of spectral analysis, we have successfully performed the first measurements of the spectra associated with the extra-weak spontaneous chemiluminences accompanied by various kinds of biochemical processes, including enzymatic reactions, autoxidations and so on. To the best of our knowledge, no spectral information of such ultra-low spontaneous chemiluminescence has been reported up to the present.

Figure 7 illustrates the measured distribution of the chemiluminescence spectrum accompanied by the decomposition of 30% hydrogen peroxide in an alkali solution of phosphate

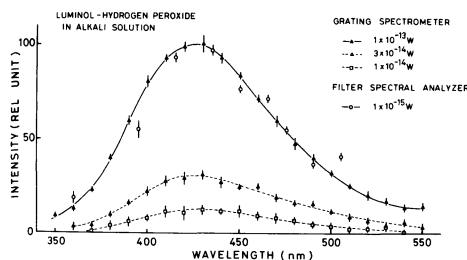


Fig. 6. Measured spectral distribution of spontaneous chemiluminescence in luminol-hydrogen peroxide system by means of the filter spectral analyzer and a conventional grating spectrometer. Comparison of the relative distribution is made between the spectrum measured at the total intensity of 10^{-15} W for the former, and that at 10^{-13} W for the latter. Another two data corresponding to the total intensity of 3×10^{-14} and 10^{-14} W are plotted on the same scale with that for 10^{-13} W obtained by the grating spectrometer.

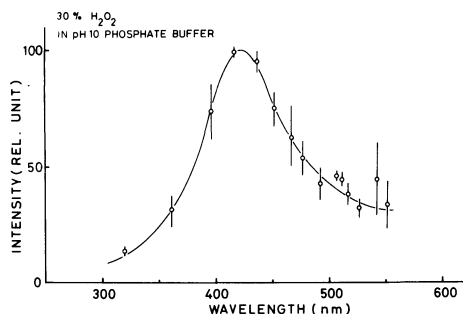


Fig. 7. Measured spectrum of the ultra-weak spontaneous chemiluminescence accompanied by decomposition of a 30% hydrogen peroxide in alkali solution of phosphate buffer with pH 10, of which the total intensity is of the order of 10^{-16} W.

buffer with pH 10, of which the total intensity was of the order of 10^{-16} W. There was found an emission band covering from near uv to yellow regions centered at around 420 nm.

Figures 8 and 9 also show typical chemiluminescence spectra involved in some enzymatic reactions such as the sodium linolate-lipoxidase and the microsomal lipoxygenation systems. In Fig. 8, the spectral measurement of the chemiluminescence from the sodium linolate-lipoxidase system is shown where the peak of the emission band is observed near 630 nm. On the other hand, in Fig. 9, the solid line shows the measured chemiluminescence spectrum with the emission band centered around 630 nm which resulted from a NADPH- Fe^{3+} -ADP-lipoproteins-cytochrome c reductase system,¹⁸⁾ while the dashed line shows the one indicating a weak emission band near 520 nm and the

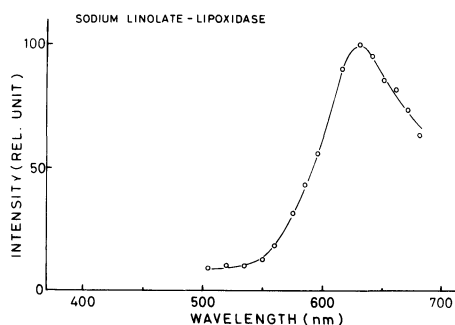


Fig. 8. Result of spectral analysis of the ultra-weak chemiluminescence inherent to the sodium linolate-lipoxidase system, of which the total intensity is estimated to be of the order of 6×10^{-15} W.

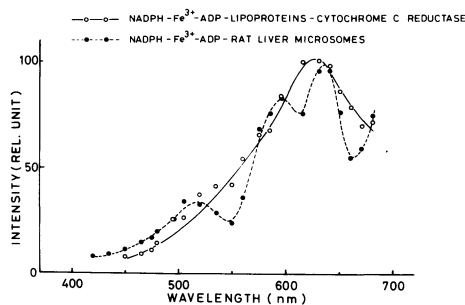
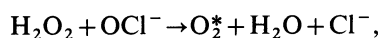


Fig. 9. Measured spectral distributions of the ultra-weak chemiluminescence associated with the NADPH- Fe^{3+} -ADP-lipoproteins-cytochrome c reductase system shown by the solid line and with the NADPH- Fe^{3+} -ADP-rat liver microsomes system shown by the dashed line, of which the total intensities are of the order of 4×10^{-15} W and 8×10^{-16} W, respectively.

prominent band near 630 nm with a shoulder of some spectral structures around 580 nm accompanied by a NADPH-Fe³⁺-ADP-rat liver microsomes system. Here, as the lipoproteins are refined from the rat liver microsomes, the former system is more purified than the latter system. The total intensities of these spectra are estimated to be of the order of 10⁻¹⁵–10⁻¹⁶ W. It is known that the common characteristic of the above reaction systems which result in chemiluminescence is that oxygen molecules are participating essentially with the process.¹⁹⁾

It is well established that the singlet oxygen molecules are produced by the reaction of the hydrogen peroxide-hypochlorite alkaline aqueous system²⁰⁾ such as



where O₂^{*} represents the oxygen molecule excited in ¹Δ_g and ¹Σ_g⁺ metastable states. These singlet oxygen molecules yield the prominent red chemiluminescence, which has very weak structures at 535, 578 and 786 nm corresponding to the (2,0), (1,0) and (0,2) vibrational bands as well as at 633.4 and 703.2 nm assigned as the (0,0) and (0,1) vibrational bands invoking the simultaneous transition in pairs of excited singlet oxygen molecules 2(¹Δ_g)→2(³Σ_g⁻). Also, there is a very weak green chemiluminescence band at 478 nm as the (0,0) band of the simultaneous pair transition (¹Σ_g⁺ + ¹Δ_g)→2(³Σ_g⁻). Moreover, the (0,0), ..., (3,0) vibronic components of the oxygen pair transition 2(¹Σ_g⁺)←2(³Σ_g⁻) are reported by the measurement of the absorption spectrum of gaseous oxygen molecules at 150 atm in the region of 300–400 nm.²⁰⁾ In the reaction involved in the hydrogen peroxide-hypochlorite system, sensitized luminescence experiments clearly indicate that the double molecule state 2(¹Σ_g⁺) exists with a finite probability of the excitation.²⁰⁾ According to these interpretations, we can expect that the (0,0), (0,1) and (0,2) bands of the simultaneous pair transition 2(¹Σ_g⁺)→2(³Σ_g⁻) will be able to provide the chemiluminescence bands located around 381.1, 405.3 and 431.5 nm, respectively.

Hence, the observed ultra-weak chemiluminescence band shown in Fig. 7 is considered to correspond to the simultaneous transition 2(¹Σ_g⁺)(0)→2(³Σ_g⁻)(0,1 or 2), and the 630 nm component in the chemiluminescence spectra

depicted in Fig. 8 and by the solid line in Fig. 9 is interpreted as being due to the simultaneous transition of the pair state 2(¹Δ_g)(0)→2(³Σ_g⁻)(0). Furthermore, the structure detected in the ultra-weak chemiluminescence in the microsomal lipoxygenation system shown by the dashed line in Fig. 9 appears to be associated with the simultaneous pair transition 2(¹Δ_g)(2,1 or 0)→2(³Σ_g⁻)(0). Even though the characteristic emission band at 703.2 nm corresponding to the simultaneous transition 2(¹Δ_g)(0)→2(³Σ_g⁻)(1) could not be confirmed owing to the wavelength limitation of the colored glass filters used in the filter spectral analyzer, the large increase of the emission intensity from 660 to 680 nm may suggest the possible existence of a (0→1) band transition.

§5. Conclusion

Experimental and analytical studies and their comparisons on the performance and the sensitivity of photoelectric methods for measuring very weak light signals based on the analog and digital techniques were performed from a unified point of view. The single photoelectron counting (SPC) and the synchronous single photoelectron counting (SSPC) methods were found to have advantages over the other methods with regard to both the signal-to-noise ratio and the effective range for receiving light energy, as far as the measurement of ultra-low light intensity was concerned.

As a further extension of these results, the method for analyzing spectral information carried in very weak light signals was investigated. On the basis of this study, the filter spectral analyzer employing a set of colored glass filters was designed and constructed to allow the optical transmission through the whole system to be as large as possible. Experimental tests aimed at examining the characteristics of this spectral analyzer and comparisons of the signal-to-noise ratio with a conventional grating spectrometer were performed by accomplishing the spectral measurement of low-level light sources with well-known spectral distributions. As a consequence, this apparatus was found to be superior by about two orders of magnitude with respect to the signal-to-noise ratio to the grating spectrometer in sacrifice of the spectral resolution.

As a potential field for applying this method

of the spectral analysis, we have performed successfully the first time measurements of extra-weak chemiluminescence spectra associated inherently with various kinds of chemical process such as enzymatic reactions and autoxidations, of which the total intensities are of the order of 10^{-15} – 10^{-16} W. Through the inspection of the measured spectra, it may be surprising to find that the various types of singlet oxygen molecules, although it depends upon each process of the reaction, appear to be participating essentially with these extra-weak chemiluminescences. This measuring method and its results could be expected widely to give valuable information and also to shed light on the new aspect of the biochemical reactions and biophysical processes in connection with ultra-low spontaneous bioluminescence.²¹⁾

We are still actively continuing the detection of very weak light emission in chemi- and bioluminescence processes and their spectral analyses including many kinds of enzymatic reactions and living tissues, not only for basic research but also for the practical applications in bioscience and medical electronics. A series of these results will be published elsewhere in the future.

Acknowledgement

The authors are grateful for the collaboration of Dr. M. Nakano, Department of Biochemistry, School of Medicine, Gunma University in performing the experiments involving the sodium linolate-lipoxidase and microsomal lipoxygenation systems. Acknowledgement should also be highly extended to the Japan Spectroscopic Co., Ltd., Tokyo for their helpful contributions in designing and constructing the filter spectral analyzer.

References

- 1) H. Inaba, N. Kaneko and T. Ichimura: IEEE J. Quantum Electronics **QE-5** (1969) 14.
- 2) H. Inaba and N. Kaneko: *Abstract ICO. Conf. Opt. Instrum. and Tech., Reading, England, 1969.*
- 3) H. Inaba, T. Ichimura, Y. Shimizu and K. Asai: *Digest Sixth Int. Quantum Electronics Conf., Kyoto, 1970*, p. 74.
- 4) T. Ichimura and H. Inaba: Oyo Buturi **39** (1970) 913 [in Japanese].
- 5) Y. Shimizu, H. Inaba, K. Kumaki, K. Mizuno, S. Hata and S. Tomioka: IEEE Trans Instrum. Meas. **IM-22** (1973) 153.
- 6) Y. Shimizu and H. Inaba: Bunkō Kenkyū **22** (1973) 195 [in Japanese].
- 7) Y. H. Pao, R. N. Zitter and J. E. Griffiths: J. Opt. Soc. Amer. **56** (1966) 1133.
- 8) Y. H. Pao and J. E. Griffiths: J. chem. Phys. **46** (1967) 1671.
- 9) C. A. Morton: Appl. Optics **7** (1968) 1.
- 10) M. L. Franklin, G. Horlick and H. V. Malmstadt: Anal. Chem. **41** (1969) 2.
- 11) R. D. Moore and O. C. Chaykovsky: Princeton Appl. Res. Tech. Bull. **109** (1963) 1.
- 12) J. Cleary: J. Opt. Soc. Amer. **57** (1967) 841.
- 13) F. T. Arecchi, E. Gatti and A. Sona: Rev. sci. Instrum. **37** (1966) 942.
- 14) C. J. Oliver and E. R. Pike: J. Phys. D: Appl. Phys. **1** (1968) 1459.
- 15) R. R. Alfano and N. Ockman: J. Opt. Soc. Amer. **58** (1968) 90.
- 16) K. Nakamura and S. E. Schwarz: Appl. Optics **7** (1968) 1073.
- 17) N. Born and E. Wolf: *Principles of Optics* (Pergamon, London, 1970) 4th ed., Chap. 4.
- 18) M. Nakano, T. Noguchi, Y. Tsutsumi, K. Sugioka, Y. Shimizu, Y. Tsuji and H. Inaba: to be published in Proc. Soc. Exp. Biol. Med. (1974).
- 19) S. D. Aust, D. L. Roerig and T. C. Pederson: Biochem. Biophys. Res. Commun. **47** (1972) 1133.
- 20) A. U. Khan and M. Kasha: J. Amer. Chem. Soc. **92** (1970) 3293.
- 21) G. M. Barenboim, A. N. Domanskii, and K. K. Turoverov: *Luminescence of Biopolymers and Cells* (Plenum, New York, 1969) p. 114.